PHYSICAL REVIEW B **96**, 161104(R) (2017)

Chiral flat bands: Existence, engineering, and stability

Ajith Ramachandran, Alexei Andreanov, and Sergej Flach
Center for Theoretical Physics of Complex Systems, Institute for Basic Science (IBS), Daejeon 34051, Republic of Korea
(Received 7 June 2017; published 9 October 2017)

We study flat bands in bipartite tight-binding networks with discrete translational invariance. Chiral flat bands with chiral symmetry eigenenergy $E = 0$ and host compact localized eigenstates for finite range hopping. For a bipartite network with a majority sublattice chiral flat bands emerge. We present a simple generating principle of chiral flat-band networks and as a showcase add to the previously observed cases a number of new potentially realizable chiral flat bands in various lattice dimensions. Chiral symmetry respecting network perturbations—including disorder and synthetic magnetic fields—preserve both the flat band and the modified compact localized states. Chiral flat bands are spectrally protected by gaps and pseudogaps in the presence of disorder due to Griffiths effects.

DOI: 10.1103/PhysRevB.96.161104

Hermitian tight-binding translationally invariant lattices with the eigenvalue problem $E\Psi_l = -\sum_m t_{lm}\Psi_m$ and certain local symmetries have been shown to sustain one or a few completely dispersionless bands, called flat bands (FBs) in their band structure [1]. The interest in FBs is due to the macroscopic degeneracy they host. Almost any perturbation will lift that degeneracy and thus lead to interesting new physics: ground-state ferromagnetism [2], unusual localization [3,4], Landau-Zener Bloch oscillations [5], to name a few examples. Thus, it is important to know which conditions have to be satisfied in order to obtain FBs, yet in practical situations it will suffice to be close enough to an ideal FB case in order to potentially realize new states of quantum matter. Flat bands with finite range hoppings rely on the existence of a macroscopic number of degenerate compact localized eigenstates (CLS) $\{\Psi_l\}$ at the FB energy E_{FB} which have strictly zero amplitudes outside a finite region of the lattice due to destructive interference [6]. Flat-band networks have been proposed in one, two, and three dimensions and various flat band generators were identified [7,8], which harvest on local symmetries. A recent systematic attempt to classify flat band networks through the properties of CLS was used to obtain a systematic flat band network generator for one-dimensional two-band networks [9]. Experimental observations of FBs and CLS are reported in photonic waveguide networks [10–15], exciton-polariton condensates [16–18], and ultracold atomic condensates [19,20]. FBs are obtained through a proper fine-tuning of the network parameters. For experimental realizations, the understanding and usage of FB protecting symmetries is therefore of high priority.

The interplay of flat bands (or equivalently, CLS) and additional symmetries was discussed in few publications so far, which mostly focused on specific models. Nongapped flat bands in a dice lattice model as a consequence of the underlying chiral symmetry was reported by Sutherland [21], as well as possible generalizations, that we work out and extend in the present work. Bound states in the continuum protected by chiral symmetry of a lattice with flat bands, were studied by Mur-Petit and Molina [22]. Poli *et al.* [23] examined the effect of partial breaking of chiral symmetry in a two-dimensional Lieb lattice, which destroyed the flat band. Leykam *et al.* [24] studied the one-dimensional diamond chain with on-site disorder which is a case of weakly broken chiral symmetry, and observed a finite localization length for states at the flat-band energy, as opposed to strict compact localization in the case of preserved chiral symmetry (see below). Green *et al.* [25] speculated that time-reversal symmetry has to be broken to gap away the flat band from dispersive bands, which might be relevant in the presence of interactions. We show below that gapped chiral FBs do not require broken time-reversal symmetry. Recently, Read analyzed the existence of CLS and, therefore, flat bands, and their relation to general topological properties for generic Hamiltonians belonging to the ten symmetry classes using algebraic K theory [26]. Below, we thoroughly explore the implications of the chiral symmetry on the existence and properties of flat bands.

Bipartite lattices separate into two A,B sublattices such that $E\Psi_l^{A,B} = -\sum_m t_{lm}\Psi_m^{B,A}$ and possess *chiral symmetry* (CS): if $\{\Psi^A,\Psi^B\}$ is an eigenvector to eigenenergy E, then $\{\mp\Psi^A, \pm\Psi^B\}$ is an eigenvector to eigenenergy $-E$. We study chiral flat bands (CFBs) with $E_{FB} = 0$ in such systems, and the ways the chiral symmetry is protecting them. Lieb's theorem [27] implies that chiral lattices with an odd number of bands always possess at least one chiral flat band, and we present a general method to compute the total number of CFBs. This allows us to derive a simple CFB network generating principle in various lattice dimensions. Disorder (or other perturbations) which preserve CS also preserve the CFB, and we show that CLS survive up to modifications. CFBs are generically gapped away from other spectral parts; however, the gap is replaced by a pseudogap in case of hopping disorder due to Griffiths effects [28].

We start with a reminder of a well-known theorem on the existence of zero-energy states for bipartite lattices [21,27]. It states that if the number N_A of the majority A-sublattice sites is larger than the corresponding number N_B of the minority B sublattice, then there are at least $\Delta N = |N_A - N_B|$ states $\{\Psi^A,0\}$ at energy $E = 0$ [21,27], which occupy the majority sublattice only.

These results naturally lead to the systematic classification of chiral flat bands: Consider a translationally invariant d-dimensional bipartite lattice, odd number ν of sites per unit cells, and $1 \leqslant \mu_B < \mu_A < \nu$. The μ_A A sites in any unit cell are only connected with nonzero hopping terms t_{lm} to the remaining μ_B B sites (possibly belonging to other unit cells). The general band structure is given by dispersion relations

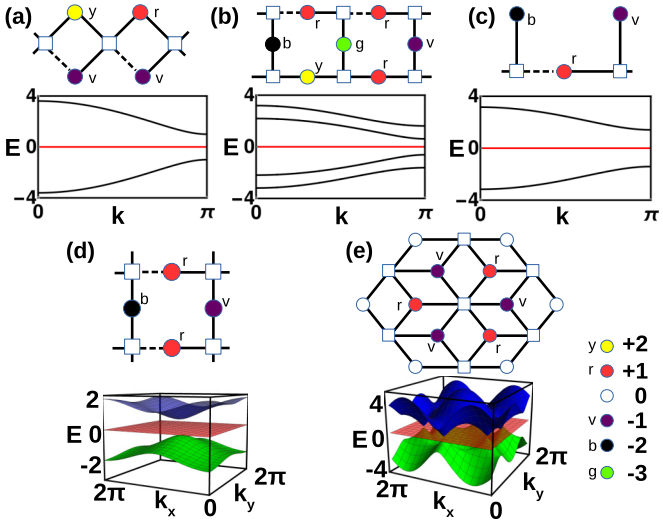

FIG. 1. Modifications of known CFB networks and their band structure (see, e.g., [1,6]). Majority and minority sublattice sites are shown with circles and squares, respectively. Solid lines: $t = 1$; dashed lines: $t = 2$. CLS amplitudes (not normalized) are shown in color code. (a) Diamond, (b) $1d$ Lieb, (c) stub, (d) 2D Lieb, and (e) $\mathcal{T}_3$ (dice).

$E_\mu(\vec{k})$ with the band index $\mu = 1, \ldots, \nu$ and $\vec{k}$ a d-component Bloch vector scanning the Brillouin zone. It follows already by general CS that at least one of the bands must either cross $E = 0$ (finite number of zero energy states) or be a FB at $E = 0$ (macroscopic number of zero-energy states), since any band which does not cross $E = 0$ is either positive or negative valued, and has a symmetry related partner band. Due to the odd number of bands, there is at least one *unpaired* band which therefore must transform into itself under CS action. In the following, we focus on a Hermitian system, but the concepts can be carried over to non-Hermitian systems as well. Further, since ν is odd, the difference in the number of sites on the A and B sublattices $\Delta N = N_{uc}(2\mu_A - \nu) \neq 0$, where $N_{uc} \sim L^d$ is the number of unit cells, and L is the linear dimension. This implies a macroscopic degeneracy at $E = 0$, which is only possible with precisely $(2\mu_A - \nu)$ FBs at $E = 0$. This observation suggests a natural classification of CFBs by the imbalance of minority and majority sites, and will be used for a CFB generator as we illustrate below. Therefore, by fixing the space dimension and the Bravais lattice, and looping over the number of sites ν and the number of sites of the majority sublattice μ_A as well as the hopping range, one can systematically explore all the possible chiral flat-band models.

We now illustrate the first few steps in this classification: Let us first discuss $d = 1$. For $\nu = 3$ there is only one possibility $\mu_A = 2$. A known example is the diamond chain structure shown in Fig. 1(a). The cutting of one bond leads to the stub structure, Fig. 1(c). For $\nu = 5$ there are two possibilities: $\mu_A = 3,4$. The case $\mu_A = 3$ leads to a generalized Lieb structure, Fig. 1(b). Cutting a bond produces a generalized *stub3* lattice, Fig. 2(b). The second case $\mu_A = 4$ arrives at a new network structure which we coin *double diamond* chain [Fig. 2(a)].

For the $d = 2$ and $\nu = 3$ case the only partitioning is again $\mu_A = 2$, yet there are different choices of Bravais lattices. For the tetragonal Bravais lattice we find a generalized 2D Lieb structure [Fig. 1(d)]. The hexagonal Bravais lattice yields, e.g., the $\mathcal{T}_3$ or dice lattice [21,29,30] [Fig. 1(e)]. Cutting two bonds in each unit cell of the $\mathcal{T}_3$ lattice yields a novel *2D stub* lattice [Fig. 2(c)]. For $\nu = 5$, there are again two partitionings, $\mu_A = 3,4$. The case $\mu_A = 3$ leads to an edge-centered honeycomb lattice [31]. In the second case $\mu_A = 4$ with three CFBs and two dispersive bands [decorated Lieb lattice, Fig. 2(d)]. For $d = 3$ and $\nu = 3$ we obtain a novel generalized *3D Lieb* structure (Fig. 3).

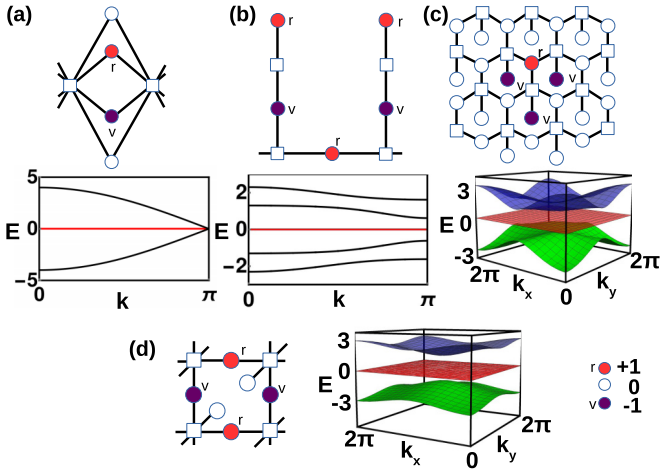

FIG. 2. Novel CFB examples (with dispersion relations). Majority and minority sublattice sites are shown with circles and squares, respectively. CLS amplitudes (not normalized) are shown in color code. (a) Double diamond, (b) stub3, (c) 2D stub, and (d) decorated Lieb.

The above approach can be extended to larger odd band numbers. Further, the approach is not restricted to odd band numbers only. Any even band number $\nu \geqslant 4$ works as well, as long as $\mu_A > \mu_B$. For instance, $\mu_A = 3$ and $\mu_B = 1$ is the first nontrivial CFB case with the smallest number of four bands,

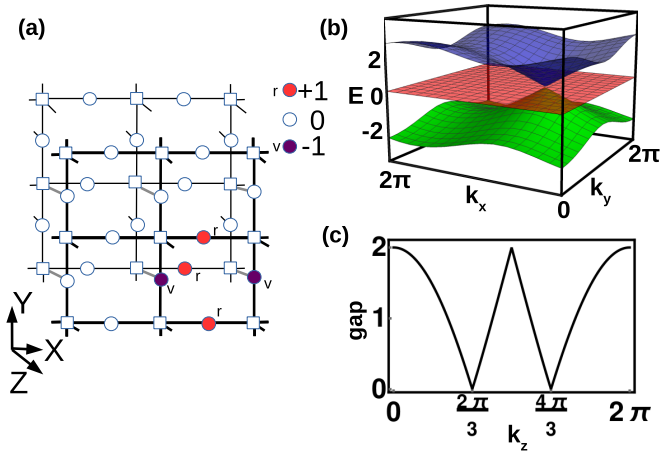

FIG. 3. A $d = 3$ CFB example of the generalized 3D Lieb structure (with dispersion relation at fixed $k_z = 2\pi/3$). Majority and minority sublattice sites are shown with circles and squares, respectively. CLS amplitudes (not normalized) are shown in color code.

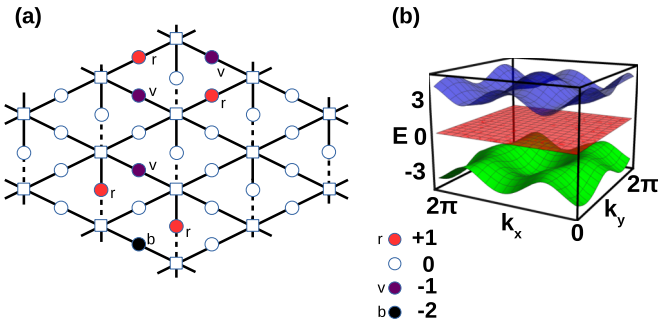

FIG. 4. A $d = 2$ CFB example with four bands and three degenerated CFBs, coined 2D RAF lattice (with dispersion relation). Majority and minority sublattice sites are shown with circles and squares, respectively. CLS amplitudes (not normalized) are shown in color code.

with two degenerated CFBs. A two-dimensional realization of such a structure is the *2D RAF* (or bond-centered triangular) structure in Fig. 4.

The most general way to generate CBFs is to simply set the numbers ν, μ_A, d and to pick a Bravais lattice. Any values of hoppings between majority and minority sublattices are allowed. The hopping range can be anything, from compact (or nearest neighbor) as chosen in the above examples, to exponentially decaying, or algebraic decaying, or not decaying at all in the lattice space. For noncompact hoppings, CLS states are not expected to persist in general and turn into exponentially, algebraically, or completely extended flat band eigenstates, since the number of equations to be satisfied turns macroscopic. Our generator therefore provides a straightforward path of generating flat bands which lack compact localized state support.

For compact or nearest-neighbor hopping it is always possible to construct a suitably sized CLS for a CFB, as follows from a simple counting of equations and variables. The nonzero CLS amplitudes must always be located on the majority sublattice and are the variables to be identified. The embedded and surrounding minority sites have amplitude zero and constitute the set of equations to be satisfied. This immediately gives an estimate of the number n_e of lattice equations to be satisfied by the CLS: $n_e = v_e L_{CLS}^d + s_e L_{CLS}^{d-1}$ and the number of variables $n_v = v_v L_{CLS}^d$. Both numbers scale proportionally to the volume L_{CLS}^d of the CLS, with $v_v > v_e$, and an equation surface contribution with some proportionality factor s_e. For large enough volume L_{CLS}^d the number of equations will always be less than the number of variables, and the CLS can be constructed. It would be interesting to combine the chiral generator with the generic CLS generator [9].

The above examples of periodic CFB structures show that in general the CFB is gapped away from dispersive bands. While for some cases we observe conical intersections at $E = 0$ and zero gaps, this happens for highly symmetric hopping parameter sets (e.g., like all hoppings equal). We checked that all models discussed above show gap openings upon changing the hopping values in the corresponding sets (without destroying the network class and periodicity). This is due to removal of accidental degeneracy of states from dispersive bands. Dispersive bands in CS networks are symmetry related, and can touch at zero energy only for discrete sets of wave-vector values. These touchings (not crossings) are additional degeneracies which are removed by perturbations, even those that respect CS. The CFB, however, remains at zero energy.

Conical intersection points in two-dimensional chiral networks without majority sublattices ($\mu_A = \mu_B$) are known to be protected by the very chiral symmetry. Indeed, in this case the Hamiltonian in k space is taking the form $H(k) = \left(\begin{smallmatrix} 0 & \mathcal{T}(k) \\ \mathcal{T}^\dagger(k) & 0 \end{smallmatrix}\right)$ where $\mathcal{T}(k)$ is a square matrix of rank $\mu_A = \mu_B$. Conical intersection points in $H(K)$ are protected since the zeros of the analytical function $\det \mathcal{T}(k)$ [and hence the zero modes of $\mathcal{T}(k)$] survive under small perturbations of the hoppings.

However, in the case of CFBs $\mu_A \neq \mu_B$ and therefore $\mathcal{T}(k)$ is a rectangular matrix. Yet we can always represent a CFB Hamiltonian in the form

$$H(k) = \begin{pmatrix} \mathcal{D}_1(k) & \mathcal{Q}(k) & 0 \\ \mathcal{Q}^\dagger(k) & \mathcal{D}_2(k) & 0 \\ 0 & 0 & E_{FB} \end{pmatrix}. \tag{1}$$

In order to have a symmetry protected conical intersection point, we have to request bipartite symmetry in the subsystem of the dispersive states, i.e., $\mathcal{D}_{1,2}(k) = 0$. That results in μ_B functions of k which have to vanish, with only a finite number of variables (the hopping set) at hand. Therefore the conical intersections observed for CFB are not protected by symmetry, although they might be preserved upon perturbations along a subset of the hopping control parameter space.

The CFB is protected even when destroying translational invariance while keeping CS. This can be easily done by randomizing the hoppings, e.g., using random uncorrelated and uniformly distributed variables $\epsilon_{ij} \in [-W/2, W/2]$ such that $t_{ij} \to t_{ij}(1 + \epsilon_{ij})$. We first consider the 1D diamond chain from Fig. 1(a) with $W = 10$, which is much larger than the gap of the ordered case, and would be expected to smear out the gap completely. Figure 5 shows the density of states for this case. We clearly observe a persistent and protected CFB with $\rho(0) = \infty$ due to flat bands and pseudogap behavior $\rho(E \to 0) \to E^\alpha$ with model dependent exponent α. The CLS persist and have a structure similar to the clean case shown in Figs. 1 and 2 but with amplitudes which are derived from the random hopping values t_{ij} which are connecting CLS sites with the minority sublattice. Consequently, CLS are now different in different parts of the chain. In Fig. 5 we show the analogous results for the 2D Lieb lattice. Again the CFB is protected by a gap, and CLS states persist, which have a structure similar to the one shown in Fig. 1(d). Finally, in Fig. 5 we show the density of states for the disordered $\mathcal{T}_3$ lattice. Clearly in all the above cases the CFB persists in the presence of symmetry preserving hopping disorder, and is protected from other states. Notably the gap is smeared and replaced by a pseudogap due to Griffiths effects, due to rare regions that are almost translationally invariant or contain conical intersections. The pseudogap scaling close to $E = 0$ is shown in the inset in Fig. 5.

In order to demonstrate the importance of the chiral symmetry protection, we computed densities of states for

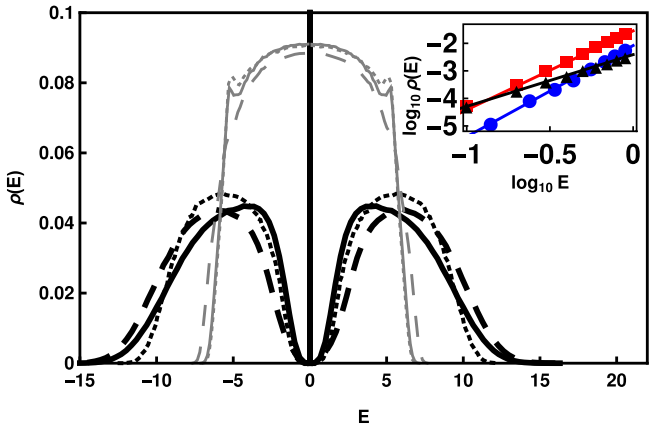

FIG. 5. The density of states $\rho(E)$ versus energy E for disordered CFB networks (see text for details): The thick black curves in the main plot show the density of states for the diamond chain (solid line), 2D Lieb lattice (dashed line), and T_3 lattice (dotted line) in the presence of CS preserving hopping disorder. The thin gray curves in the main plot show the density of states for the same systems, but in the presence of CS breaking on-site disorder. Clearly the FB is destroyed, densities turn finite, and the Lifshitz tails are removed. The inset shows the details of the vanishing of the density of states for small but nonzero energies [log-log plots for diamond chain (red squares), 2D Lieb (blue circles), and $\mathcal{T}_3$ (black triangles) lattice].

the modified eigenvalue problem, $(E-\epsilon_l)\Psi_l = -\sum_m t_{lm}\Psi_m$, with diagonal (on-site) disorder. The random uncorrelated on-site energies ϵ_l break the CS and the CFB is destroyed, and the pseudogap and δ peak at $E=0$ are smeared (Fig. 5).

Finally, let us discuss the possibility of linear dependence of the CLS. To enforce linear dependence of the set of all CLS, we need to zero at least one linear combination of them, which leads to $N\mu_A$ equations with only N variables (coefficients) available. This is in general impossible, unless additional constraints are met. Therefore the set of all CLS is generically linearly independent and spans the entire Hilbert space of the CFB.

That is at variance with flat bands in systems lacking chiral symmetries, e.g., for the kagome and 2D pyrochlore (checkerboard) lattices [24]. In these cases, the CLS set is linearly dependent [32]. The search for one missing state leads to the existence of two different compact localized lines. The unexpected additional state at the flat band energy is therefore due to band touching. A similar linear dependence of the CLS set happens also for nongapped CFBs, e.g., for the 2D Lieb lattice with all hoppings being equal, or for the dice lattice in Fig. 1. Reducing the symmetry in the hopping network $\{t_{lm}\}$ while keeping the chiral symmetry preserves the flat band, opens a gap, and turns the CLS set into a linearly independent one. It is an interesting question whether similar reductions of the symmetry of the hopping networks for nonchiral systems with band touchings will preserve the flat band, gap it away from dispersive states, and make the CLS set complete.

Turning the hopping matrix elements complex will destroy time-reversal symmetry, and may correspond to the introduction of synthetic magnetic fields in the context of Bose-Einstein condensates [33–40], and of light propagation in waveguide networks [41,42]. These changes preserve CS and therefore, the CFB persists also together with the CLS. This has been shown for the one-dimensional diamond chain in Ref. [5], where a magnetic field preserves the CFB, the CLS, and opens a gap. Further, we can even leave Hermitian grounds and consider dissipative couplings [43]. Still the CFB will be protected due to the above reasoning of having a majority sublattice. Therefore CFBs can be realized even in dissipative non-Hermitian settings.

To conclude, we presented the theory of chiral flat bands. We study flat bands in chiral bipartite tight-binding networks with discrete translational invariance. Chiral flat bands are located at the chiral symmetry eigenenergy $E=0$ and host compact localized eigenstates. For a bipartite network with a majority sublattice degenerated chiral flat bands exist. We derived a simple generating principle of chiral flat band networks and illustrated the method by adding to the previously observed cases a number of new potentially realizable chiral flat bands in various lattice dimensions. We have also pointed out the possible constructions of flat-band models with no CLS. Chiral symmetry respecting network perturbations—including disorder, synthetic magnetic fields, and even non-Hermitian extensions—preserve the flat band and compact localized states, which are only modified. Chiral flat bands are thus protected; however, the gaps are replaced by pseudogaps in the presence of disorder, due to the contribution of rare regions.

ACKNOWLEDGMENTS

S.F. thanks H. Schomerus for useful discussions. This work was supported by the Institute for Basic Science, Project Code IBS-R024-D1.

[1] O. Derzhko, J. Richter, and M. Maksymenko, Strongly correlated flat-band systems: The route from Heisenberg spins to Hubbard electrons, Int. J. Mod. Phys. B **29**, 1530007 (2015).

[2] M. Maksymenko, A. Honecker, R. Moessner, J. Richter, and O. Derzhko, Flat-Band Ferromagnetism as a Pauli-Correlated Percolation Problem, Phys. Rev. Lett. **109**, 096404 (2012).

[3] C. Danieli, J. D. Bodyfelt, and S. Flach, Flat-band engineering of mobility edges, Phys. Rev. B **91**, 235134 (2015).

[4] J. D. Bodyfelt, D. Leykam, C. Danieli, X. Yu, and S. Flach, Flatbands Under Correlated Perturbations, Phys. Rev. Lett. **113**, 236403 (2014).

[5] R. Khomeriki and S. Flach, Landau-Zener Bloch Oscillations with Perturbed Flat Bands, Phys. Rev. Lett. **116**, 245301 (2016).

[6] S. Flach, D. Leykam, J. D. Bodyfelt, P. Matthies, and A. S. Desyatnikov, Detangling flat bands into Fano lattices, Europhys. Lett. **105**, 30001 (2014).

[7] A. Mielke, Ferromagnetism in the Hubbard model on line graphs and further considerations, J. Phys. A **24**, 3311 (1991).

[8] H. Tasaki, Ferromagnetism in the Hubbard Models with Degenerate Single-Electron Ground States, Phys. Rev. Lett. **69**, 1608 (1992).

[9] W. Maimaiti, A. Andreanov, H. C. Park, O. Gendelman, and S. Flach, Compact localized states and flat-band generators in one dimension, Phys. Rev. B **95**, 115135 (2017).

[10] D. Guzmán-Silva, C. Mejía-Cortés, M. A. Bandres, M. C. Rechtsman, S. Weimann, S. Nolte, M. Segev, A. Szameit, and R. A. Vicencio, Experimental observation of bulk and edge transport in photonic Lieb lattices, New J. Phys. **16**, 063061 (2014).

[11] R. A. Vicencio, C. Cantillano, L. Morales-Inostroza, B. Real, C. Mejía-Cortés, S. Weimann, A. Szameit, and M. I. Molina, Observation of Localized States in Lieb Photonic Lattices, Phys. Rev. Lett. **114**, 245503 (2015).

[12] S. Mukherjee, A. Spracklen, D. Choudhury, N. Goldman, P. Öhberg, E. Andersson, and R. R. Thomson, Observation of a Localized Flat-Band State in a Photonic Lieb Lattice, Phys. Rev. Lett. **114**, 245504 (2015).

[13] S. Mukherjee and R. R. Thomson, Observation of localized flat-band modes in a quasi-one-dimensional photonic rhombic lattice, Opt. Lett. **40**, 5443 (2015).

[14] S. Weimann, L. Morales-Inostroza, B. Real, C. Cantillano, A. Szameit, and R. A. Vicencio, Transport in sawtooth photonic lattices, Opt. Lett. **41**, 2414 (2016).

[15] S. Xia, Y. Hu, D. Song, Y. Zong, L. Tang, and Z. Chen, Demonstration of flat-band image transmission in optically induced Lieb photonic lattices, Opt. Lett. **41**, 1435 (2016).

[16] N. Masumoto, N. Y. Kim, T. Byrnes, K. Kusudo, A. Löffler, S. Höfling, A. Forchel, and Y. Yamamoto, Exciton–polariton condensates with flat bands in a two-dimensional kagome lattice, New J. Phys. **14**, 065002 (2012).

[17] F. Baboux, L. Ge, T. Jacqmin, M. Biondi, E. Galopin, A. Lemaître, L. Le Gratiet, I. Sagnes, S. Schmidt, H. E. Türeci, A. Amo, and J. Bloch, Bosonic Condensation and Disorder-Induced Localization in a Flat Band, Phys. Rev. Lett. **116**, 066402 (2016).

[18] C. E. Whittaker, E. Cancellieri, P. M. Walker, D. R. Gulevich, H. Schomerus, D. Vaitiekus, B. Royall, D. M. Whittaker, E. Clarke, I. V. Iorsh, I. A. Shelykh, M. S. Skolnick, and D. N. Krizhanovskii, Exciton-polaritons in a two-dimensional Lieb lattice with spin-orbit coupling, arXiv:1705.03006.

[19] S. Taie, H. Ozawa, T. Ichinose, T. Nishio, S. Nakajima, and Y. Takahashi, Coherent driving and freezing of bosonic matter wave in an optical Lieb lattice, Sci. Adv. **1**, e1500854 (2015).

[20] G.-B. Jo, J. Guzman, C. K. Thomas, P. Hosur, A. Vishwanath, and D. M. Stamper-Kurn, Ultracold Atoms in a Tunable Optical Kagome Lattice, Phys. Rev. Lett. **108**, 045305 (2012).

[21] B. Sutherland, Localization of electronic wave functions due to local topology, Phys. Rev. B **34**, 5208 (1986).

[22] J. Mur-Petit and R. A. Molina, Chiral bound states in the continuum, Phys. Rev. B **90**, 035434 (2014).

[23] C. Poli, H. Schomerus, M. Bellec, U. Kuhl, and F. Mortessagne, Partial chiral symmetry-breaking as a route to spectrally isolated topological defect states in two-dimensional artificial materials, 2D Mater. **4**, 025008 (2017).

[24] D. Leykam, J. D. Bodyfelt, A. S. Desyatnikov, and S. Flach, Localization of weakly disordered flat band states, Eur. Phys. J. B **90**, 1 (2017).

[25] D. Green, L. Santos, and C. Chamon, Isolated flat bands and spin-1 conical bands in two-dimensional lattices, Phys. Rev. B **82**, 075104 (2010).

[26] N. Read, Compactly supported Wannier functions and algebraic K theory, Phys. Rev. B **95**, 115309 (2017).

[27] E. H. Lieb, Two Theorems on the Hubbard Model, Phys. Rev. Lett. **62**, 1201 (1989).

[28] R. B. Griffiths, Nonanalytic Behavior Above the Critical Point in a Random Ising Ferromagnet, Phys. Rev. Lett. **23**, 17 (1969).

[29] J. Vidal, R. Mosseri, and B. Douçot, Aharonov-Bohm Cages in Two-Dimensional Structures, Phys. Rev. Lett. **81**, 5888 (1998).

[30] J. Vidal, P. Butaud, B. Douçot, and R. Mosseri, Disorder and interactions in Aharonov-Bohm cages, Phys. Rev. B **64**, 155306 (2001).

[31] Z. Lan, N. Goldman, and P. Öhberg, Coexistence of spin-$\frac{1}{2}$ and spin-1 Dirac-Weyl fermions in the edge-centered honeycomb lattice, Phys. Rev. B **85**, 155451 (2012).

[32] D. L. Bergman, C. Wu, and L. Balents, Band touching from real-space topology in frustrated hopping models, Phys. Rev. B **78**, 125104 (2008).

[33] Y.-J. Lin, R. L. Compton, A. R. Perry, W. D. Phillips, J. V. Porto, and I. B. Spielman, Bose-Einstein Condensate in a Uniform Light-Induced Vector Potential, Phys. Rev. Lett. **102**, 130401 (2009).

[34] Y. J. Lin, R. L. Compton, K. Jimenez-Garcia, J. V. Porto, and I. B. Spielman, Synthetic magnetic fields for ultracold neutral atoms, Nature (London) **462**, 628 (2009).

[35] M. Aidelsburger, M. Atala, M. Lohse, J. T. Barreiro, B. Paredes, and I. Bloch, Realization of the Hofstadter Hamiltonian with Ultracold Atoms in Optical Lattices, Phys. Rev. Lett. **111**, 185301 (2013).

[36] H. Miyake, G. A. Siviloglou, C. J. Kennedy, W. C. Burton, and W. Ketterle, Realizing the Harper Hamiltonian with Laser-Assisted Tunneling in Optical Lattices, Phys. Rev. Lett. **111**, 185302 (2013).

[37] M. Aidelsburger, M. Lohse, C. Schweizer, M. Atala, J. T. Barreiro, S. Nascimbene, N. R. Cooper, I. Bloch, and N. Goldman, Measuring the Chern number of Hofstadter bands with ultracold bosonic atoms, Nat. Phys. **11**, 162 (2014).

[38] I. Bloch, J. Dalibard, and S. Nascimbene, Quantum simulations with ultracold quantum gases, Nat. Phys. **8**, 267 (2012).

[39] J. Struck, C. Ölschläger, M. Weinberg, P. Hauke, J. Simonet, A. Eckardt, M. Lewenstein, K. Sengstock, and P. Windpassinger, Tunable Gauge Potential for Neutral and Spinless Particles in Driven Optical Lattices, Phys. Rev. Lett. **108**, 225304 (2012).

[40] A. Celi, P. Massignan, J. Ruseckas, N. Goldman, I. B. Spielman, G. Juzeliūnas, and M. Lewenstein, Synthetic Gauge Fields in Synthetic Dimensions, Phys. Rev. Lett. **112**, 043001 (2014).

[41] M. Golshani, S. Weimann, Kh. Jafari, M. K. Nezhad, A. Langari, A. R. Bahrampour, T. Eichelkraut, S. M. Mahdavi, and A. Szameit, Impact of Loss on the Wave Dynamics in Photonic Waveguide Lattices, Phys. Rev. Lett. **113**, 123903 (2014).

[42] S. Longhi, Effective magnetic fields for photons in waveguide and coupled resonator lattices, Opt. Lett. **38**, 3570 (2013).

[43] D. Leykam, S. Flach, and Y. D. Chong, Flat bands in lattices with non-hermitian coupling, Phys. Rev. B **96**, 064305 (2017).